

This is an Open Access document downloaded from ORCA, Cardiff University's institutional repository:<https://orca.cardiff.ac.uk/id/eprint/126590/>

This is the author's version of a work that was submitted to / accepted for publication.

Citation for final published version:

Zeinalipour-Yazdi, Constantinos D. and Catlow, C. Richard A. 2019. An experimental and computational IR and hybrid DFT-D3 study of the conformations of l-lactic and acrylic acid: new insight into the dehydration mechanism of lactic acid to acrylic acid. *Physical Chemistry Chemical Physics* 21 (40) , pp. 22331-22346. 10.1039/C9CP02968K

Publishers page: <http://dx.doi.org/10.1039/C9CP02968K>

Please note:

Changes made as a result of publishing processes such as copy-editing, formatting and page numbers may not be reflected in this version. For the definitive version of this publication, please refer to the published source. You are advised to consult the publisher's version if you wish to cite this paper.

This version is being made available in accordance with publisher policies. See <http://orca.cf.ac.uk/policies.html> for usage policies. Copyright and moral rights for publications made available in ORCA are retained by the copyright holders.



An experimental and computational IR and hybrid DFT-D3 study of the conformations of L-lactic and acrylic acid: new insight into the dehydration mechanism of lactic acid to acrylic acid

Constantinos D. Zeinalipour-Yazdi *^{abc} and C. Richard A. Catlow^{abd}

We have studied using hybrid Density Functional Theory (DFT) with an aug-cc-pVTZ basis set and D3 dispersion corrections the intra-molecular hydrogen bond of L-lactic acid and L-lactic-acid analogs with the hydroxyl group on the alpha carbon atom substituted by a-XH (where X = S, Se, Te) as well as the conformations of acrylic acid. The results show that there are three types of intramolecular hydrogen bonds that can form only when a-OH is present, whereas other less electronegative functional groups such as –SH, –SeH and –TeH do not exhibit the formation of an intramolecular H-bond. We show that the intra-molecular H-bond formed between the alpha-OH hydrogen and the COOH carbonyl oxygen would enhance the rate of nucleophilic substitution of alpha-OH at the K⁺ sites in the previously suggested dehydration mechanism of L-lactic to acrylic acids. We find that a temperature range between 190 and 210 °C would be optimum to maximise the rate of nucleophilic substitution of the alpha-OH group at the potassium sites during the dehydration mechanism of L-lactic acid to acrylic acid. Additionally, our hybrid-DFT simulation of the infrared spectrum of the various conformers shows that the lowest energy conformer can be identified by a single vibrational band at 3734 cm⁻¹ whereas for the other conformers, this vibrational band is split with Dn that ranges between 6 cm⁻¹ and 176 cm⁻¹. We also find that the various conformers of acrylic acid can be identified by a double peak for the C=O and O–H vibrations, which have Dn⁰ and Dn⁰⁰ values of 24 and 42 cm⁻¹, respectively. This computational study is useful for spectroscopic experimental efforts that try to identify the various conformers of L-lactic acid and acrylic acid and to gain mechanistic insight into the dehydration mechanism over K substituted NaY zeolites.

Introduction

The industrial production of lactic acid (α-hydroxypropionic) occurs via bacterial fermentation of sugar and starch that contain carbohydrates or by chemical synthesis from acetaldehyde that originates from coal and crude oil.¹ Bacterial fermentation can produce racemic lactic acid consisting of a 1 : 1 mixture of D- and L-stereoisomers or even 99.9% L-lactic acid. L-Lactate, the conjugate base of lactic acid, is constantly produced in animals from pyruvate via the enzyme lactate dehydrogenase (LDH) in a process of fermentation during normal metabolism and exercise.

The main industrial use of lactic acid is for the manufacturing of polylactic acid (PLA). Polymer derivatives of lactic acid are biocompatible and biodegradable and are therefore used in medical devices, implants and drug delivery systems.^{2,3} The global annual production of lactic acid was 260 000 tons (excluding PLA) in 2008 and in 2020, it is estimated to be 1 000 000 tons for lactic acid and PLA.⁴ Clearly, there is an increasing need for eco-friendly packaging and there will be a huge market potential in coming years for lactic acid derived plastics.

The dehydration of lactic acid to acrylic acid depicted in Fig. 1 is a very important reaction in the development of green routes for its utilisation, as acrylic acids and their esters are primary building blocks for all acrylate polymers and plastics.^{5–7} Therefore, the discovery of a catalyst that can efficiently produce acrylic acid from a renewable source is very desirable and would have a significant economic and environmental impact. Currently, industry uses the direct oxidation of propene to produce acrylic acid for which the catalytic dehydration of lactic acid to acrylic acid could become a

^aDepartment of Chemistry, University College London, 20 Gordon Street, London, WC1H 0AJ, UK

^bUK Catalysis Hub, Research Complex at Harwell, Rutherford Appleton Labs, Harwell Campus, OX11 0FA, UK

^cSchool of Science, University of Greenwich, Central Avenue, Chatham Maritime, Kent ME4 4TB, UK. E-mail: c.zeinalipouryazdi@greenwich.ac.uk

^dSchool of Chemistry, Cardiff University, Park Place, Cardiff, CF10 1AD, UK

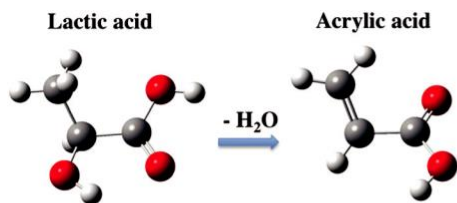


Fig. 1 Figure showing the dehydration of lactic acid to acrylic acid.

tantalizing ‘green’ alternative.⁷ The catalytic conversion of lactic acid to acrylic acid has been shown to be possible with heterogeneous catalysts, such as phosphate impregnated metal oxides, with moderate yields (40–58 mol%).⁸ Higher yields of 61 mol% have been reported by a base treated calcinated aluminum phosphate catalyst at a reaction temperature of 320–375 °C.⁹ KX-modified NaY zeolites have also been found to catalyze the dehydration of lactic acid to acrylic acid and a mechanism has been proposed.¹⁰ In this mechanism, the lactic acid adsorbs to the potassium cation coordinating through its hydroxyl (–OH) moiety whereas a hydrogen (–H) from the methyl group interacts with the oxygen of a Si–O–Al moiety. These interactions lead to the abstraction of –OH and –H causing acrylic acid to desorb whereas the former adsorbates recombine on the surface of the catalysts forming water, which when desorbs, regenerates the catalytic site.¹⁰

Understanding the dynamic conformational changes of L-lactic acid as a function of temperature is critical in understanding its adsorption and dehydration mechanism. It has been previously found by van Eijck that lactic acid forms an intramolecular hydrogen bond between the α-hydroxyl group and C=O of a carboxylate group (conformer D in Fig. 2) using microwave spectroscopy in the gas phase.¹¹ Using the semi-empirical AM1 and SCF/3-21G method, Norris and Gready found 9 conformers for lactic acid with the lowest energy conformer being the one where the α-OH bond was intramolecularly H-bonded to the OH group of the carboxylic acid (conformer C in Fig. 2).¹² Formation of the hydrogen bond leads to a stabilisation of 10.4 kcal mol⁻¹.¹³ Spectroscopic evidence of two higher energy conformers comes from Fausto and co-workers through matrix isolated Fourier transform-infrared (IR) spectroscopy and theoretical calculations at the DFT(B3LYP)/6-311G(d,p) and MP2/6-31G(d,p) levels of theory, which showed that conformer D is the lowest energy structure.^{14,15} The same group also studied the structure of lactic acid oligomers (i.e. dimers, trimers and tetramers) using B3LYP/6-311++G(d,p) supported by IR and ¹H/¹³C NMR studies, which found that the most stabilising intermolecular interaction is the O–H...O bond.¹⁶ Banerjee et al. calculated the pK_a value for lactic acid using B3LYP/SMD and M06-2X/SMD and found that it is 16 using MeOH as a reference (see ref. 17).

In this study, we have performed a systematic study using hybrid dispersion-corrected DFT (DFT-D3) of the various H-bonds that form in L-lactic acid and three analogs of lactic acid that have less electronegative elements at the alpha hydroxyl group. First, in Section 1.1, we evaluate the temperature at which there is rotational freedom of the carboxylate

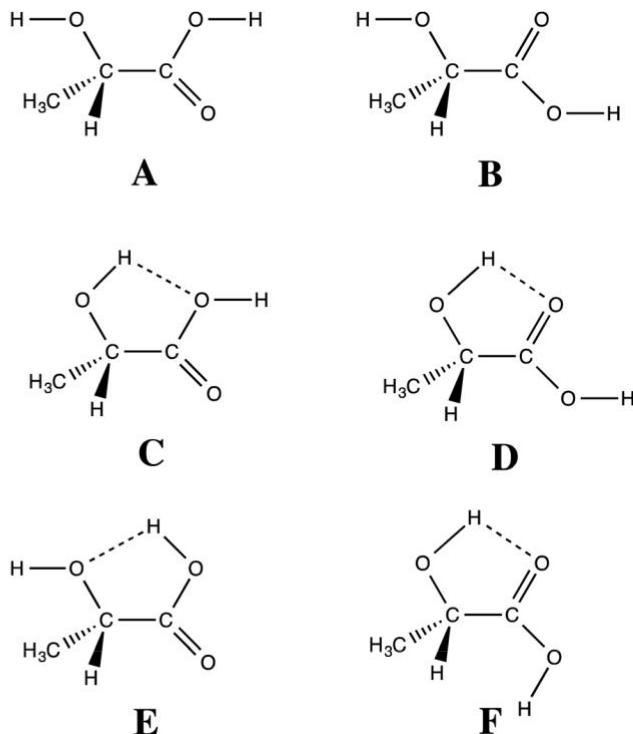


Fig. 2 Various local and global minima of L-lactic acid found using the B3LYP-D3/aug-cc-pVTZ method.

group. We calculate the relative free energy change with respect to the lowest energy conformer. In Section 1.2, we examine the effect of the electronegativity of the hydroxyl group on the formation of the hydrogen bond. In Section 1.3, we simulate the infrared absorption spectrum of the various conformers of lactic acid and suggest a way that the formation of the H-bond can be experimentally confirmed. In Section 1.4, we study the effect of the basis set on the calculated vibrational frequencies. In Section 1.5, we identify the various conformers of L-lactic acid using IR spectroscopy simulations. In Section 1.6, we study the various conformers of acrylic acid and in Section 1.7, we make an assignment of the vibrational bands in their infrared absorption spectra.

Computational methods

DFT calculations have been performed with Gaussian 09¹⁸ with the use of Becke’s three-parameter hybrid exchange functional¹⁹ (XC) combined with the Lee–Yang–Parr non-local correlation functional,²⁰ abbreviated as B3LYP. The B3LYP exchange–correlation functional was appropriate, as this would yield accurate oscillator frequencies in modelling IR spectra of adsorbate–metal cluster systems.^{21–23} For the basis functions, we have used the spherical version (5d, 7f), the correlation consistent augmented valence triple zeta basis set,^{24–28} abbreviated as aug-cc-pVTZ for C, O, S, Se and H and the ECP-121G basis set for Te. Dispersion forces were accounted for with the D3 method by Grimme as implemented in Gaussian 09. The level of theory is abbreviated as B3LYP-D3/ECP-121G(Te), aug-cc-pVTZ(C,O,S,Se,H).

Lactic acid was fully optimised and the stationary points were confirmed using vibrational analysis, by the absence of imaginary vibrational frequencies. The SCF convergence criteria for the root mean square (RMS) density matrix and the total energy were set to 10^{-8} Hartrees/Bohr and 10^{-6} Hartrees, respectively.

The simulated IR spectra were predicted within the harmonic oscillator approximation where the intensity of each vibrational mode i was taken to be proportional to the square of the derivative of the molecular dipole field with respect to the vibrational coordinate, q_i :

$$\frac{\partial}{\partial q_i} \left(\sum_{\alpha} \mu_{\alpha} \frac{dq_{\alpha}}{dq_i} \right)^2 \quad (1)$$

where the harmonic oscillator wavefunctions are used for $v=0$ and $v=1$. We have calculated the dipole derivatives and the force constants from the DFT wavefunction.²⁹

Results and discussion

The study of conformational changes in L-lactic acid and acrylic acid is important to understand better their mechanism of interconversion. Intra-molecular H-bonds can affect the conformational dynamics to a great extent as they stabilise intermediate conformations that maximise the strength of the intermolecular interactions. Here, we study such conformational changes in L-lactic acid and determine the temperature of interconversion of the various conformers of L-lactic acid via a simple model described in the following section.

1.1 Temperature of conformational change

Estimation of the temperature of conformational change as a function of activation barrier is derived in this section. For a general isomerisation reaction of the form $A \rightleftharpoons B$, we can say that the rate of the forward reaction is given by

$$k_A = e^{-D_{GA}/RT} \quad (2)$$

and the rate of the reverse reaction is given by

$$k_B = e^{-D_{GB}/RT} \quad (3)$$

The equilibrium quotient for this isomerisation reaction is given by

$$Q = \frac{k_A}{k_B} \quad (4)$$

So, if we substitute the Arrhenius equation into eqn (4), the reaction quotient becomes

$$Q = \exp \left(\frac{D_{GB} - D_{GA}}{RT} \right) \quad (5)$$

A reaction where all of A converts to B can be represented well by a reaction quotient that manifests that the concentration of the products is 100 times larger than the concentration of the reactants,

$$Q = 100. \quad (6)$$

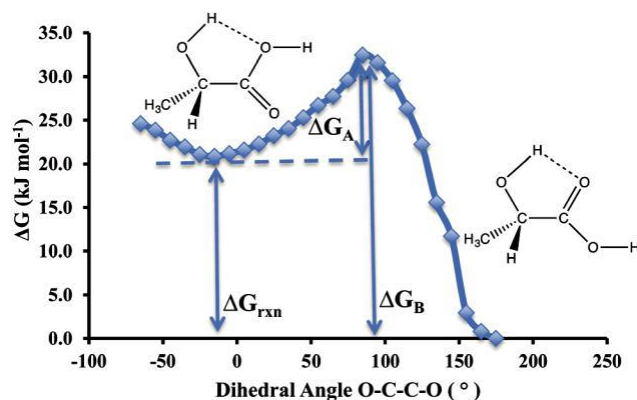


Fig. 3 Relaxed dihedral scan of O-C-C-O angle of lactic acid starting with the lowest energy conformer (i.e. D) using B3LYP-D3/aug-cc-pVTZ. All coordinates were allowed to relax apart from the O-C-C-O dihedral angle.

Substituting eqn (5) into eqn (6) and solving for the temperature yields

$$T = \frac{D_{GB} - D_{GA}}{\delta \ln Q} \quad (7)$$

Eqn (7) can give the temperature at which isomer A will turn into isomer B with a ratio of their concentrations of 1 : 99. For a single barrier process, the numerator according to Fig. 3 is just the free energy change of the isomerization reaction DG_{rxn}

$$T = \frac{DG_{rxn}}{4.6R} \quad (8)$$

We performed a relaxed dihedral scan of L-lactic acid, shown in Fig. 3, which shows that the barrier for the isomerisation of lactic acid from conformer D to C is 32.5 kJ mol^{-1} . Interestingly, there is only a single barrier separating the two isomers, which indicates that both the H-bond formation barrier and the barrier due to conformational changes of the isomers are considered in this PES and that the H-bonding barrier is more important than the conformational barrier. Furthermore, this potential energy landscape shows that reaction coordinate is indeed the dihedral angle. It is therefore evident that from eqn (8), we only have to calculate the energetic difference between the various conformers to estimate the temperature at which the isomerisation occurs.

From the Gibbs free energy change given in the last column of Table 1, we can also estimate the strength of the intra-molecular hydrogen bond formed, which is given by taking the Gibbs free energy difference between conformer D and B, which is 18.6 kJ mol^{-1} , indicative of a strong H-bond when O-H binds to a C=O group. Previous SCF/3-21G calculations¹² found that this energy difference between the two conformers is 20.9 kJ mol^{-1} , which is in good agreement with the value found here. However, their¹² ranking of the relative energies of the conformers finds that conformer C is the lowest in energy, whereas we find that conformer D is lower by 9.3 kJ mol^{-1} , which is in agreement with the lowest energy conformer found by Fausto and co-workers.¹⁴ This result clearly shows that the inclusion of electron correlation and dispersion interactions in

Table 1 Free energy change and dihedral angle for the various conformers of L-lactic acid with respect to lowest energy conformer with and without the D3-correction at B3LYP/aug-cc-pVTZ level of theory

Labels	Structural formula	d with DG			DG with D3
		d (1)	D3 (1)	(kJ mol ⁻¹)	¹) (kJ mol ⁻¹)
A		22.7	24.8	16.8	17.4
B		162.8	163.9	17.8	18.6
C		31.9	33.9	9.0	9.3
D		176.0	174.8	0.0	0.0
E		6.9	7.8	9.5	9.9
F		175.2	173.6	19.4	19.3

our study is necessary to get the correct ordering of the relative stability of the various conformers. The energetic ranking of the various conformers is identical to the order found from B3LYP calculations with a smaller basis set (i.e. 6-311++G(d,p)) and the absence of dispersion interaction correction (i.e. D3) apart from conformers B and A whose order was reversed.¹⁴ We also did not observe two versions of conformer C (i.e. GskC and G⁰sk⁰C), which in our calculations both relaxed into the H-bonded structure of conformer C.

The hydrogen bond strength of the various conformers when evaluated based on the distance of H O was found to be H–O H–OCQO (E) 4 O–H OQCOH (D) 4 O–H O–HCQO (C), which correspond to H-bond lengths of 1.929 Å, 2.120 Å and 2.302 Å, respectively. This is in agreement with the H-bonds that L-(+)-lactic acid forms in the solid state, which are entirely O–H OQCOH and H–O H–OCQO, as found from X-ray diffraction if we consider that the molecules in the crystal would adopt positions/conformations that maximise the strength of both intra-molecular and inter-molecular H-bonding interactions.³⁰

On the contrary, if we attempt to estimate the H-bond strength from the energetic difference of the various conformers, we do not get the same ordering. In particular, the energetic difference between conformers C and A suggests a H-bond strength for conformer C of 8.1 kJ mol⁻¹, whereas comparing conformer E and A, the H-bond strength of E is 7.5 kJ mol⁻¹ smaller, which is not consistent with the H-bond strength on the basis of H-bond length, which suggests that E should form a much stronger H-bond than C. This clearly suggests that apart from the H-bond formation, the isomerisation energies are affected considerably by the relative conformation of the O–C–C–O skeleton.

From the various conformers found on the potential energy surface of lactic acid, we can identify 3 different conformational processes. The first is between A and B, in which the dihedral changes by 185.51 while the O–H bonds are pointing away and not forming an intramolecular H-bond. The reaction temperature for this functional group rotational process is 31 K and therefore this rotation can occur even at room temperature (RT = 25 1C). The second is between D and C, in which the dihedral angle changes by 2091. For these two conformers, the α -hydroxyl group is hydrogen-bonded with the carboxylate carbonyl or hydroxyl group. The enthalpy change for this isomerisation is 9.3 kJ mol⁻¹, which corresponds to an isomerisation temperature of 243 K, which can happen again at RT. The third process is the breaking of the H-bond going from conformer D to B. This process is endothermic by 18.6 kJ mol⁻¹ and the temperature at which this reaction occurs efficiently is 486 K (213 1C). The last process is expected to have serious implications on the catalytic dehydration mechanism of lactic acid in NaY zeolites, as the formation of this H-bond below

213 1C enhances the partial negative charge on the α -OH oxygen, which makes it more reactive towards nucleophilic substitution reactions. In a proposed mechanism¹⁰ of the lactic acid dehydration mechanism, the α -OH group undergoes nucleophilic substitution at the cationic K⁺ substituted Na⁺ sites of the zeolite NaY, as shown in Fig. 8 of ref. 10. Similarly, on zirconia surfaces, α -OH undergoes nucleophilic substitution at Zr sites.³¹ In both cases, the nucleophilic substitution will be faster if the partial negative charge on the oxygen of the α -OH group is more negative. Therefore, the H-bond that forms between the α -OH hydrogen and the COOH carbonyl oxygen in conformer D that occurs at temperatures below

213 1C would in principle enhance the rate of the dehydration mechanism. Consequently, it is important that the intra-molecular H-bond is present during the dehydration of lactic acid, which, from our estimate of the rotational barrier of the carboxylate group, would happen for temperatures below

213 1C. However, as the temperature of the reaction decreases, the rate decreases. It is therefore evident from these computational data that the rate of the dehydration mechanism of lactic acid is maximised in a very small temperature range between 190 and 210 1C. This temperature range should assist in experimental efforts of increasing the catalytic dehydration mechanism of lactic acid over the potassium substituted zeolite NaY. A detailed modelling of the reaction mechanism in NaY

zeolites will be given elsewhere and this preliminary study is concerned mostly with IR spectral features that can assist in the identification of higher energy conformers of lactic and acrylic acid.

1.2 Effect of electronegativity of a-XH group (where X = O, S, Se, Te) on intramolecular H-bond

We investigated whether the substitution of a less electronegative atom that belongs to the same group of the periodic table has an effect on the intramolecular H-bond formation. The lactic acid-like molecules optimised using the D3-B3LYP/CEP-121G method and the D3-B3LYP/aug-cc-pVTZ method are presented in Fig. 4. The same starting structure was used for these full atom optimisations, which was the optimised structure of L-lactic acid using the latter method. Certain selected geometric parameters, such as the dihedral angle of the H-bond ($d(X-C-C-O)$) and the length of the H-bond measured as $r(H-O)$, along with the corresponding values of electronegativity of group 6 atoms are tabulated in

Table 2. From these results, we observe that $d(X-C-C-O)$, which for lactic acid is almost 180°, becomes about 90°, which causes $a(X-H)$ to become parallel with the C=O bond of the carboxylic acid and be located at a larger intramolecular separation. The larger separation can be seen by the increase of the H-O bond as a function of the decreasing electronegativity (and larger atomic radius) of the group 6 element ($X = O, S, Se, Te$). The formation of the H-bond in just lactic acid is in agreement with the textbook definition of the H-bond that indicates that a hydrogen atom that has a covalent link with one of the electronegative atoms (F, N, O) forms an electrostatic link with another electronegative atom in the same or another molecule. We therefore find that among the various lactic acid analogs with O, S, Se and Te, only the analog that has a hydroxyl group on the alpha carbon will form a strong H-bond, which can be clearly seen by the distance of

$r(H-O)$, which increases from 2.302 Å for OH to 3.077 Å for SH to 3.226 for SeH to 3.581 Å for TeH. The absence of the hydrogen

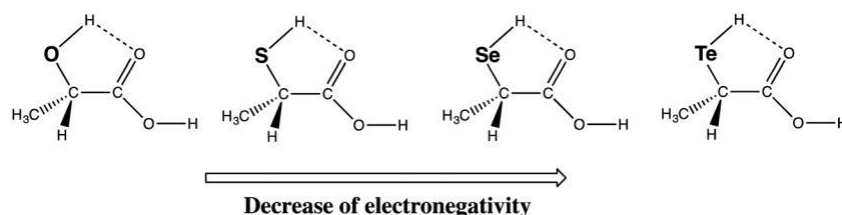


Fig. 4 Various lactic acid-like compounds examined for the formation of an intra-molecular H-bond.

Table 2 Selected geometric parameters of optimised structures of lactic acid-like compounds where a-XH (where X = O, S, Se, Te) using the B3LYP-D3/ECP-121G method (and B3LYP-D3/aug-cc-pVTZ in parenthesis)

Labels	Struc. formula	$d(X-C-C-O)$ (°)	$r(H-O)$ (Å)	H-Bond formation	Electron e.g. Pauling ³²
D ^a		164.6 (174.8)	2.302 (2.120)	Forms	3.44
F		97.3 (93.2)	3.077 (3.008)	Does not form	2.58
G		91.9 (89.7)	3.226 (3.139)	Does not form	2.55
H		86.1	3.581	Does not form	2.10

^a The H-bond strength obtained for lactic acid using the ECP-121G basis is 17.5 kJ mol⁻¹, which compares very well with the value obtained with the aug-cc-pVTZ basis set, which is 18.6 kJ mol⁻¹.

bond formation can also be observed by the value of the dihedral angle $d(X-C-C-O)$, which for XQO is about 180 degrees but for all other analogs that do not form a hydrogen bond, this dihedral becomes roughly 90 degrees.

1.3 Simulated and experimental infrared spectrum of lactic acid

A detailed analysis of the rotational isomers of lactic acid was performed by Fausto and co-workers using matrix isolated FT-IR spectroscopy and B3LYP/6-311++G(d,p) and MP2/6-31G(d,p) calculations.¹⁴ Study of the vibrational bands of L-(+)-lactic acid in the solid phase using Raman and IR spectroscopy was performed by Groshev et al. supported by B3LYP/6-31++G(d,p) calculations, which found a weak O-H bond of the carboxylic acid at 3292 cm^{-1} at 295 K.³⁴ Their calculated value for the O-H oscillator frequency (i.e. 3752 cm^{-1}) is in good agreement with the value we report here (i.e. 3734 cm^{-1}). The infrared spectrum for the lowest energy conformer of L-lactic acid was calculated in Fig. 5a using the B3LYP-D3/aug-cc-pVTZ method. The values for the frequency (ν_{IR}), intensity (I_{IR}), bond length (r) and bond angle (j) are tabulated in Table 3. The most intense bands are the carbonyl stretching $\nu(\text{C=O})$ at 1795 cm^{-1} and the hydroxyl C-OH stretching at 1139 cm^{-1} . The latter band was previously found from matrix isolated IR spectroscopy in Ar at 9 K to belong to isolated lactic acid positioned at 1120 cm^{-1} .¹⁴ This band had additional bands

in the range of $1120\text{--}1140\text{ cm}^{-1}$ that corresponded to weakly bound lactic acid water complexes and higher ordered aggregates (i.e. lactic acid dimers, trimers, etc.) monitored by varying the water percentage in the Ar matrix.¹⁴ The carbonyl stretching frequency peak was previously measured by IR and Raman in aqueous solutions of lactic acid and found to be at 1725 cm^{-1} .^{1,35} It was also measured in vibrational absorption spectroscopy experiments of L-lactic acid in CDCl_3 and found to be a double peak at 1745 cm^{-1} and 1721 cm^{-1} due to monomeric and aggregated (e.g. monomers, dimers, trimers) lactic acid, respectively.³⁶ In the experimental IR spectrum from the NIST database, shown in Fig. 5b, this peak is found at 1782 cm^{-1} . We observe that the relative position of this band depends on how free this carbonyl group is to move. In conformer B, where there is an absence of H-bonding interaction between O-H and carboxylate, this band is found at 1836 cm^{-1} . When there is a H-bonding interaction between O-H and the carboxylate O-H, there is a shift of this band to 1816 cm^{-1} , which occurs in conformer C. It is noted that this shift of the band should be observable in a highly resolved infrared spectrum. Another peak that we observe to be perturbed by the formation of the inter-molecular hydrogen bond is the vibrational peak of the hydroxyl group of $\alpha\text{-OH}$ (3726 cm^{-1}) and the O-H bond of the carboxyl group (3731 cm^{-1}). Around 3100 cm^{-1} , there are four rather weak peaks that correspond to the stretching of C-H

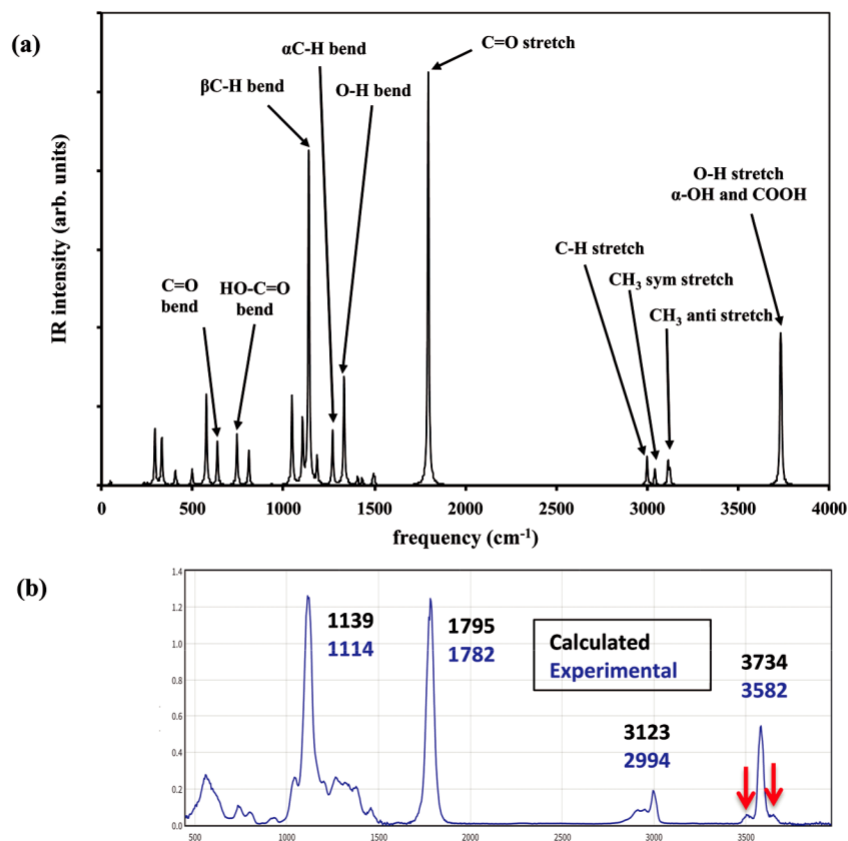


Fig. 5 (a) Calculated infrared spectrum of the lowest energy conformer (i.e. conformer D) of lactic acid using the B3LYP-D3/aug-cc-pVTZ method and (b) experimental IR spectrum of lactic acid in the gas phase.³³

Table 3 Tabulated values for the infrared frequency (ν_{IR}), infrared intensity (I_{IR}), bond length (r) and bond angle (θ) for lactic acid using the B3LYP-D3/aug-cc-pVTZ method

Vibrational mode	Frequency (cm^{-1})	Intensity ($10^{40} \text{esu}^2 \text{cm}^2$)	Bond length (\AA)	Bond angle ($^\circ$)
O–H stretch of COOH	3736	73	0.969	108
O–H stretch of a-OH	3731	93	0.967	108
C–H antisym. stretch of b-CH ₃	3123	15	1.088	109
C–H antisym. stretch of b-CH ₃	3113	23	1.088	109
C–H sym. stretch of b-CH ₃	3041	16	1.088	109
C–H stretch of a-CH	2998	28	1.096	109
CQO stretch	1795	685	1.206	124
O–H bend of a-CH and COOH	1333	249	—	—
C–H bend of a-CH	1270	126	—	—
C–OH stretch	1139	905	—	—
HO–CQO bend of COOH	744	203	—	—
CQO bend of COOH	637	206	—	—

Table 4 Comparison of experimental and calculated IR peaks for selected high intensity peaks in the IR spectrum (0 to 4000 cm^{-1}) for lactic acid

Basis on H	Basis on C and O	b C–H bend (cm^{-1})	CQO stretch (cm^{-1})	CH ₃ anti stretch ^a (cm^{-1})	O–H stretch ^a (cm^{-1})	Av. diff. (cm^{-1})
cc-pVDZ	cc-pVDZ	1152	1820	3129	3690	79.8
cc-pVDZ	aug-cc-pVDZ	1140	1791	3132	3735	81.5
cc-pVDZ	aug-cc-pVTZ	1139	1795	3108	3724	73.5
aug-cc-pVDZ	aug-cc-pVTZ	1138	1795	3109	3726	74.0
aug-cc-pVTZ	aug-cc-pVTZ	1139	1795	3123	3734	79.8
daug-cc-pVTZ	aug-cc-pVTZ	1139	1795	3123	3734	79.8
aug-cc-pVQZ	aug-cc-pVTZ	1139	1796	3116	3749	82.0
daug-cc-pVQZ	aug-cc-pVTZ	1139	1796	3116	3749	82.0
Experimental		1114	1782	2994	3582	

^a Taken as the average of two peaks.

in b-CH₃. In particular, the antisymmetric C–H stretch of b-CH₃ is found at 3123 cm^{-1} and 3113 cm^{-1} . The symmetric C–H stretch of b-CH₃ is at 3041 cm^{-1} followed by the stretching peak of C–H of a-CH found at 2998 cm^{-1} . The O–H bending mode of a-CH and COOH is found at 1333 cm^{-1} followed by the bending peak of C–H of a-CH (1270 cm^{-1}) and the stretching frequency of C–OH (1139 cm^{-1}). The lowest frequency peaks are the bending modes of the COOH group. In particular, the bending of the angle of HO–CQO is at 744 cm^{-1} and that of the CQO group is at 637 cm^{-1} . A complete list of these peaks and their intensities as well as selected geometric parameters is given in Table 3.

1.4 Effect of basis set on vibrational frequencies

It is common to scale calculated IR frequencies in an IR spectrum by a scale factor to lower their values by 3–7%. Usually calculated frequencies are scaled down by this scale factor to take into account limitations of the basis set used, anharmonicity effects and the partial neglect of electron correlation. The well resolved peak in our calculated IR spectrum that shows the best agreement with experiment is the CQO stretching band at 1795 cm^{-1} . Based on the position of this band in our calculated infrared absorption spectrum and the peak that corresponds to monomeric lactic acid, we have calculated a frequency scale factor of 0.993. However, we notice that certain peaks agree better than others in the calculated IR spectrum compared to the experimental IR spectrum of lactic acid that was recorded in the gas phase. The C–H bend peak of b-CH₃ (exp. 1114 cm^{-1} , calc. 1139 cm^{-1}) is in relatively good agreement

with the calculated value at B3LYP-D3/aug-cc-pVTZ. The peaks that involve the stretching of O–H bonds, such as the C–H antisymmetric stretch of b-CH₃ (3123 cm^{-1}) and the O–H stretching frequency (3734 cm^{-1}), overestimate the IR peaks considerably. We have performed a series of calculations with split basis sets on C, O and H to understand whether this difference observed mainly for the C–H and O–H stretching frequencies could be attributed to the basis set. The results of using a split basis set are shown in Table 4.

The average difference (D_x) between experimental IR and theoretical IR peaks is given by

$$D_x = \frac{1}{n} \sum_{i=1}^n \frac{|x_{\text{exp}} - x_{\text{calc}}|}{x_{\text{calc}}} \quad (9)$$

We observe that D_x between calculated and experimental peaks ranges between 73.5 and 82.0 cm^{-1} . Therefore, we do not observe a significant effect of the basis set on the vibrational frequencies when Dunning's correlation-consistent basis sets are used. The aug-cc-pVTZ basis set generates a good result for vibrations that involve C and O. The D_x of 73.5 cm^{-1} is found when a cc-pVDZ basis set is used on H. So, we recommend that if a split basis set is used, cc-pVDZ(H)/aug-cc-pVTZ(C,O) seems to be the best compromise between computational accuracy and computational demand and it reproduces best the experimental IR bands with a frequency scale factor of 0.993. The existing average difference between experimental and calculated vibrational frequencies could be due to anharmonicity effects that have not been considered in this study as we were

mostly concerned with frequency differences (i.e. $\Delta\nu$) in which such anharmonic corrections would not significantly alter the values.

1.5 Identification of various conformers of lactic acid from the IR spectrum

It is useful to be able to identify the various conformers of L-lactic acid from experiment as this could offer the means of studying aspects of the reaction mechanism under in situ conditions. In Fig. 6, we zoom-in on the IR spectrum of the various conformers of lactic acid for the peaks that correspond to the vibration of the two hydroxyl groups. In all conformers, this peak is a doublet, where the peak of the alpha hydroxyl group is higher in frequency by $\Delta\nu$, which is shown in Table 5, along with the frequencies of O–H of the alpha hydroxyl group ($\nu(\text{OH1})$) and the carboxylate group ($\nu(\text{OH2})$). However, for conformer D, this doublet peak turns into a single peak since the vibrational frequencies are at 3731 and 3736 cm^{-1} , with a $\Delta\nu$ of only 5 cm^{-1} . The same peak that corresponds to $\nu(\text{O–H})$ in the gas phase spectrum of lactic acid is a single peak, confirming the dominating occurrence of conformer D, in agreement with the relative stability of the various conformers as presented in Table 1. Closer observation of the experimental gas phase IR spectrum shown in Fig. 5b shows that there are additional peaks (shown by the red arrows) lower and higher in wavenumber than the main peak at 3582 cm^{-1} . The weak peak at lower frequencies (i.e. to the left of the main peak at 3582 cm^{-1}) could in principle be an overtone ($\nu = 2$) band of the $\nu(\text{C=O})$ band (i.e. $2 \times 1782 = 3564 \text{ cm}^{-1}$) or bands that arise due to H-bonds between lactic acid dimers. However, the weak peak that appears at higher frequencies of the main peak at 3582 cm^{-1} cannot be rationalised based on previous arguments. This peak therefore is consistent with the presence of the additional conformers of lactic acid in the gas phase. We therefore suggest that the O–H stretching band should be re-evaluated in experimental IR spectra for the presence of additional conformers. Yet the resolution of the experimental IR spectrum from the NIST database does not resolve the individual $\nu(\text{O–H})$ peaks for the six different

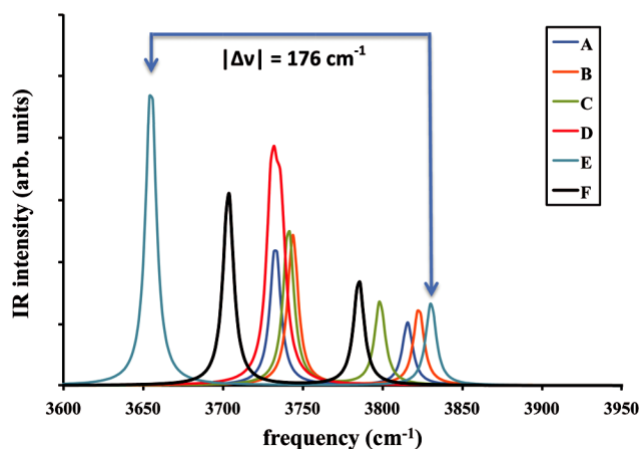


Fig. 6 Calculated infrared spectrum showing O–H vibrations of conformers A–F of lactic acid using the B3LYP-D3/aug-cc-pVTZ method.

conformers, which may be possible with higher-resolution IR spectrometers. Evidence which supports the existence of additional conformers in the O–H stretching frequency peak comes from the relative separation of the weak peaks adjacent to the main peak at 3582 cm^{-1} . In particular, from the experimental spectrum and by fitting 3 Gaussian functions, we find that $\Delta\nu$ is 152 cm^{-1} , which is in good agreement with the maximum $\Delta\nu$ of 176 cm^{-1} that we find from the calculated IR spectra of L-lactic acid. Based on the relative energetic ordering of the various conformers and their $\Delta\nu$ values shown in Fig. 6, we estimate that the additional peaks of the other conformers that are present in the experimental spectrum are the peaks of conformer C and conformer E, both of which are 9 kJ mol^{-1} higher in energy than the lowest energy conformer D. Therefore, the relative energetic ordering of the various conformers and their appearance in the IR spectrum are in good agreement.

As future development of the resolution of these spectroscopic techniques may allow identification of the individual peaks of each conformer, we have tabulated in Table 5 a list of all the vibrational frequencies, the O–H bond length and their intensities for the two hydroxyl groups as well as their separation, $\Delta\nu = \nu(\text{OH1}) - \nu(\text{OH2})$.

In the analysis of the O–H bond length and vibrational frequencies, we find a trend that is consistent with the formation of H-bonds. This comes in addition to the evidence that comes from the dihedral angle shown in Table 1 and from the relative orientation that the O–H group has with respect to the adjacent OQ or OH group of the carboxyl group. From the data presented in Table 5, it is evident that the formation of the intra-molecular H-bond has an effect on the length of the O–H bond, which can be clearly seen in Fig. 7. In particular, we observe that the formation of the H-bond can be confirmed by a lengthening of O–H compared to the same O–H bond in the non H-bonded conformer. In Fig. 7, the H-bonded bond lengths are shown by a green circle and these bonds are all smaller than the corresponding non H-bonded O–H bonds. Additionally, we observe a linear correlation between the length of the O–H bond and its vibrational frequency, which suggests that the vibrational frequency of the O–H bond can be used as a descriptor to assess the existence of such intra-molecular H-bonds on the basis of spectroscopic data.

The data in Fig. 7 nicely show that there is an inverse correlation between the length of the O–H bond and its vibrational frequency. Furthermore, they show that different O–H groups have plots that are shifted by a constant, however the slope of these plots is the same. We therefore use this correlation to identify the formation of hydrogen bonds in the various conformers, which are shown as a green circle in Fig. 7.³⁷ For both lines presented in Fig. 7, all the H-bonded conformers have the longest O–H bond lengths for the bond length belonging to the same kind of O–H bond.

1.6 DFT-D3 study of various conformers of acrylic acid

Near-infrared (NIR) spectroscopy and anharmonic DFT calculations were used to investigate propionic acid, butyric acid, acrylic acid, crotonic acid and vinylacetic acid, which suggested

Table 5 Vibrational frequencies and intensities of the O–H vibrational peaks and their absolute wavenumber separation $|D_n|$ calculated at the B3LYP/aug-cc-pVTZ level of theory

Labels	Structural formula	$\nu(\text{OH1})$ [$r(\text{OH1})$] (cm^{-1}) (\AA)	$I(\text{OH1})$ ($10^{-40} \text{esu}^2 \text{cm}^2$)	$\nu(\text{OH2})$ [$r(\text{OH2})$] (cm^{-1}) (\AA)	$I(\text{OH2})$ ($10^{-40} \text{esu}^2 \text{cm}^2$)	D_n (cm^{-1})
A		3816 [0.962]	30.8	3733 [0.969]	71.0	83
B		3823 [0.962]	38.0	3744 [0.968]	75.0	79
C		3799 [0.963]	41.4	3741 [0.968]	79.4	57
D		3731 [0.967]	92.8	3736 [0.969]	73.5	6
E		3831 [0.961]	40.6	3655 [0.973]	156.1	176
F		3703 [0.969]	91.0	3785 [0.965]	52.1	82

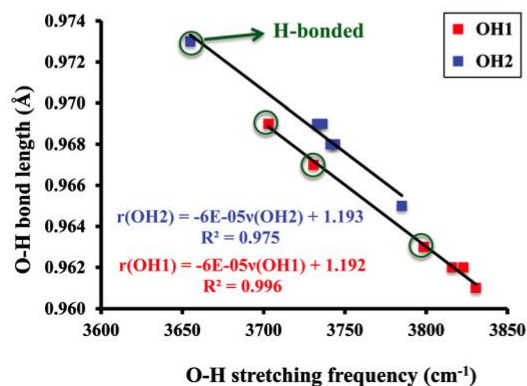


Fig. 7 Plot of O–H bond length as a function of the vibrational frequency of the O–H bond for the various conformers (A–G) of lactic acid using B3LYP-D3/aug-cc-pVTZ.

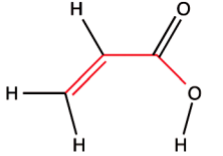
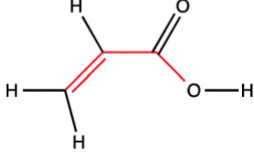
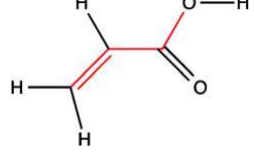
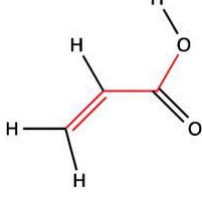
that the terminal CQC bond leads to the appearance of highly specific NIR bands.³⁸

We now consider the conformational landscape of acrylic acid. In Table 6, we have calculated at the B3LYP-D3/aug-cc-pVTZ level of theory the various conformers of the molecule. We find that there are a total of 4 conformers (J–M), which are the result of the rotation of the carboxylate group and the hydrogen of the hydroxyl group. The lowest energy conformer is

conformer L, which has a C–C–O–H dihedral angle of 180° and is therefore a completely planar molecule identical to the structure found from B3LYP/6-31(d,p) calculations.³⁹ Furthermore, the energetic ordering of the four conformers is identical to the ordering obtained at a lower level of theory HF/6-31G*//3-21G, however the energy differences vary considerably.⁴⁰ All other conformers except conformer J are planar due to the better overlap of the p-orbitals of the {CQCz and {CQO bonds. In conformer J, there is a steric repulsion between H of the O–H group and C–H of the vinyl group, which forces the geometry of the molecule out of planarity, and the dihedral of C–C–O–H becomes 18.91°. This steric repulsion can be estimated by the relative energy of conformers J and K to be about 22 kJ mol⁻¹.

In conformer M, we observe a steric repulsion of the hydrogen of the O–H group and the hydrogen of the vinyl group as the latter O–H bond is not completely parallel to the C–H bond. It is interesting that although there are steric repulsions, the molecule still has a planar configuration, which is a direct result of the delocalised nature of the p-bonds along the CQC–CQO skeleton. The existence of comparable amounts of conformer L (s-cis) and conformer K (s-trans) has been previously suggested based on microwave spectroscopic measurements of acrylic acid vapors at low pressures.^{41,42} This observation agrees well with the fact that the relative stability of the two rotational conformers is very

Table 6 Free energy change for the various conformers of acrylic acid and their dihedral angle with and without the D3-correction at B3LYP/aug-cc-pVTZ level of theory

Labels	Structural formula	d with DG (kJ mol ⁻¹)		DG with D3 (kJ mol ⁻¹)
		(1)	D3 (1)	
J		16.9	18.9 23.3	23.2
K		0.0	0.0 1.4	1.3
L		180.0	180.0 0.0	0.0
M		180.0	180.0 21.1	21.1

similar with a DG value of just 1.3 kJ mol⁻¹. Previous theoretical studies of acrylates (i.e. acrolein, acrylic acid, methyl acrylate) using the HF/6-31G*/3-21G method found that the s-cis conformation is slightly favoured over the s-trans conformation.⁴⁰ Studies of the infrared spectrum of solid acrylic acid showed that the molecule dimerises forming mostly cis-cis and trans-trans dimers⁴³ whereas earlier studies both in liquid and in vapor assigned the IR spectroscopic features to just the trans-trans dimer.⁴⁴

From the various conformers found on the potential energy surface of acrylic acid, we can identify 4 different conformational processes. The first process is between K and L, in which the dihedral angle C-C-C-O changes by 180° while the p-conjugated system changes from trans to cis. This process has a free energy change of just 1.3 kJ mol⁻¹, which corresponds to a reaction temperature of 34 K, which is possible even at RT.

The second process is between J and M, in which the dihedral angle C-C-C-O changes by 163.11°, while the p-conjugated system changes from trans to cis. This process has a free energy change of just 2.1 kJ mol⁻¹, which corresponds to a reaction temperature of 55 K, which is possible even at RT.

The third process is one in which there is a rotation of the O-H group between conformer J and K. This process has a free energy change of 21.9 kJ mol⁻¹, which corresponds to a reaction temperature of 572 K (299 °C). The analogous rotation

of the O-H group for conformer L and M has a free energy change of 21.1 kJ mol⁻¹, which corresponds to a reaction temperature of 551 K (278 °C). It is known that conformers K and L can dimerise forming trans-trans and cis-cis acrylic acid dimers.⁴³ Based on the calculated temperatures at which the O-H group will rotate into the higher energy conformers J and M, it is conceivable that above 300 °C, the dimerisation of these dimers will not be energetically favoured, which may be important in experiments that aim to probe the conformational dynamics of the monomeric forms of acrylic acid.

1.7 Simulated and experimental infrared spectrum of acrylic acid

The infrared spectrum for the lowest energy conformer of acrylic acid was calculated in Fig. 8a using the B3LYP-D3/aug-cc-pVTZ method. The values for the frequency (ν_{IR}), intensity (I_{IR}), bond length (r) and bond angle (β) are tabulated in Table 7. The most intense band is the carbonyl stretching $\nu(C=O)$ at 1789 cm⁻¹ (exp. 1772 cm⁻¹), which appears as a double peak. The separation of the double peak in the IR spectrum of the vapour is $\Delta\nu^0 = 24$ cm⁻¹. From the calculated infrared spectrum showing the vibrational bands for C=O shown in Fig. 9a, it is clear that the doublet peak cannot be a result of the rotational isomerisation of s-cis (conformer L) to s-trans (conformer K) as their $\Delta\nu^0$ is just 2 cm⁻¹. However, $\Delta\nu^0$ between conformer K and L and that of the other high energy conformers (J and M) ranges between 24 and 36 cm⁻¹. Based on the separation of the double peak in the experimental and calculated IR spectrum, we find that the doublet peak is a result of the O-H bond pointing towards or away from the vinyl hydrogens. Close observation of the structure of O-H in conformers J and M shows that there is repulsive interaction between O-H and C-H. In conformer J, this causes the CQC-C-OH dihedral angle to become 18.91° whereas in conformer M, the C-H and O-H bonds are not completely parallel. Both these structural features indicate intra-molecular repulsive interactions, which affect the vibrational frequency of the C=O bond.

The intra-molecular repulsion that affects the vibrational frequency of the C=O bond also has an effect on the peak that corresponds to the vibration of O-H at 3585 cm⁻¹ and calculated at 3743 cm⁻¹. This peak compares well to the previous experimental assignment of 3541 cm⁻¹ based on the IR spectrum of very dilute solutions of acrylic acid in CCl₄ in which it was in monomeric form, as was evident by a broader peak that narrowed to a single peak upon dilution.⁴⁵ The differences in vibrational frequencies of the O-H bond for the various conformers of acrylic acid are shown in Fig. 9b. They indicate a $\Delta\nu^0$ of 42 cm⁻¹, which suggests considerable broadening of the O-H peak even in the absence of inter-molecular H-bonds. Indeed, the experimental IR spectrum of acrylic acid in the gas phase (see Fig. 8b) shows evidence of this peak broadening of the O-H band.

We observe that the agreement of calculated and experimental IR peaks is not as good as it is for the rest of the peaks, which can be attributed to the fact that in the gas phase, the

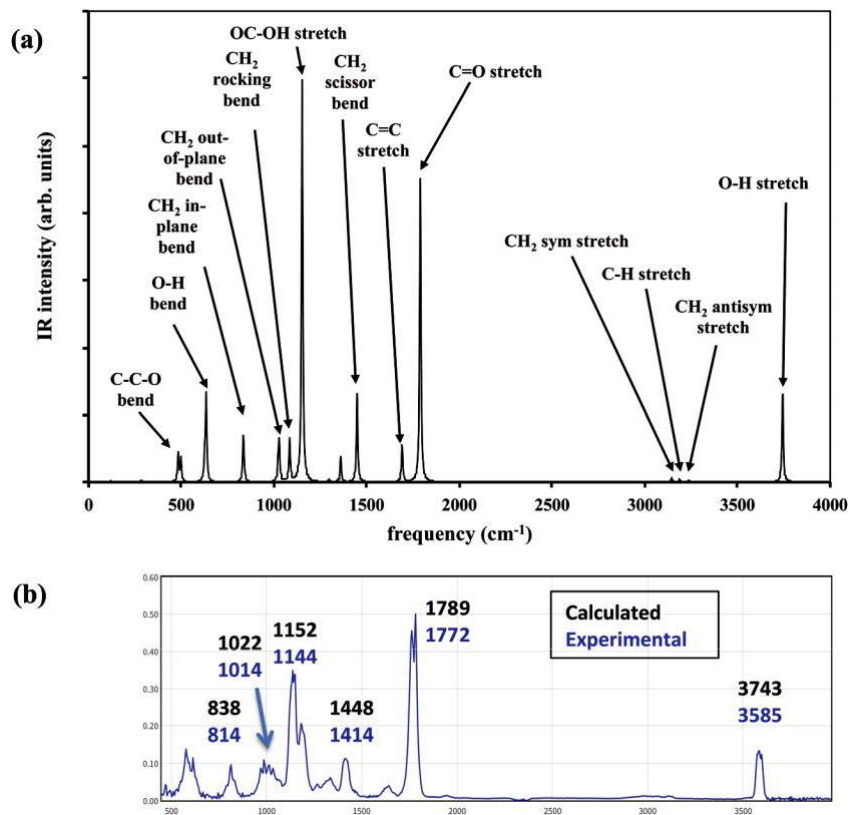


Fig. 8 (a) Calculated infrared spectrum of lowest energy conformer of acrylic acid using the B3LYP-D3/aug-cc-pVTZ method and (b) experimental IR spectrum of acrylic acid in the gas phase.³³

Table 7 Tabulated values for the infrared frequency (ν_{IR}), infrared intensity (I_{IR}), bond length (r) and bond angle (θ) for acrylic acid using the B3LYP-D3/aug-cc-pVTZ method

Vibrational mode	Frequency (cm^{-1})	Intensity ($10^{40} \text{esu}^2 \text{cm}^2$)	Bond length (\AA)	Bond angle ($^\circ$)
O-H stretch	3743	85.3	0.968	107.16
CH ₂ antisym. stretch	3238	1.3		
C-H stretch	3187	2.4		
CH ₂ sym. stretch	3145	3.7		
C=O stretch	1789 ^a	608.9	1.206	126.18
{CQCz stretch	1691	76.3	1.328	120.42
CH ₂ scissor bend	1448	76.1		
OC-OH stretch	1152	1199.9	1.357	111.14
CH ₂ rocking bend	1084	37.1		
CH ₂ out-of-plane bend	1022	14.5		
CH ₂ in-plane bend	838	37.1	1.481	
O-H bend	634	464.3		
C-C-O bend	498	163.7		

^a Average of two peaks.

oscillator strength of the O-H bond will be somewhat weaker, due to hydrogen bonding, which causes the smaller wavenumber of the experimental peak. We observe this phenomenon also for lactic acid where all peaks apart from the O-H peak have good agreement between calculated and experimental values even without frequency scaling. The next most intense band is at 1448 cm^{-1} , which corresponds to the CH₂ scissor bending vibration. The next peak, which is located at 1152 cm^{-1} , also has another peak somewhat higher in wavenumber. It is not clear what the origin of this double peak is. It could be that it

corresponds to the acrylic acid molecules that are dimerised via H-bonding as acrylic acid dimerises forming mostly cis-cis and trans-trans dimers.⁴³ It would be interesting if the concentration of monomeric and dimeric acrylic acids in the gas phase could have some effect on the relative intensity of the two peaks in order to confirm the dimerisation phenomenon. For the next band, we observe 4 peaks in the experimental spectrum but only two in the calculated spectrum. The peak with the biggest agreement is the out-of-plane bending of the CH₂ group, which is found at 1022 cm^{-1} and 1014 cm^{-1} in the experimental and calculated IR

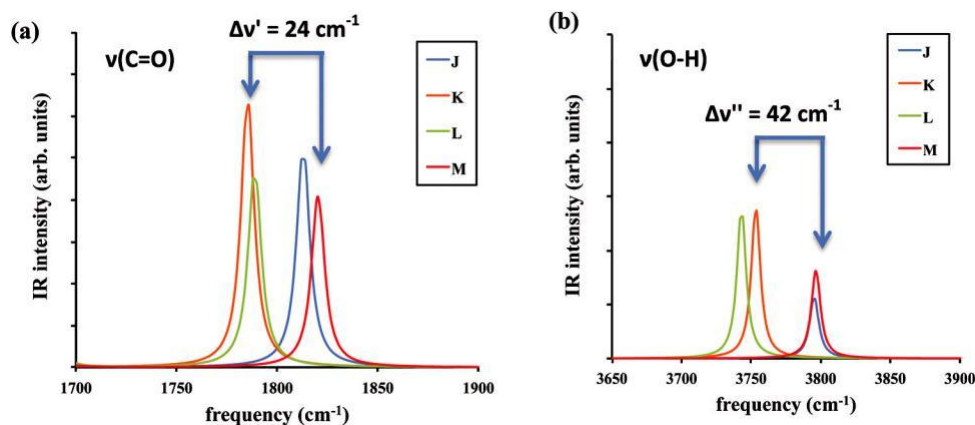


Fig. 9 (a) Calculated infrared spectrum showing (a) C=O and (b) O–H vibration of conformers J–M of acrylic acid using the B3LYP-D3/aug-cc-pVTZ method.

spectrum, respectively. The in-plane bending of the CH₂ group was found at 838 cm⁻¹ and 814 cm⁻¹ in the calculated and experimental IR spectrum, respectively. The calculated IR oscillator frequencies are on average value 18 cm⁻¹ greater than the experimental values, which shows relatively good agreement between experiment and calculation at the B3LYP-D3/aug-cc-pVTZ level of theory.

A complete list of these peaks and their intensities as well as selected geometric parameters is given in Table 7.

Conclusions

In this hybrid DFT-D3 study, we evaluate the temperatures at which the various intra-molecular H-bonds of L-lactic acid form and the conformations of acrylic acid. We find evidence that one intramolecular H-bond in L-lactic acid has an effect on the proposed reaction mechanism for L-lactic acid dehydration to acrylic acid and that there is an optimum temperature range (190–210 °C) where the catalyst turn-over-frequency would be the greatest. Furthermore, we have systematically studied the IR spectrum of L-lactic acid and acrylic acid. We have identified various characteristics that can identify the various conformers of these compounds via infrared spectroscopy. In particular, the lowest energy conformer can be identified by a single vibrational band at 3734 cm⁻¹ whereas for the other conformers, this vibrational band is split with $\Delta\nu$ that ranges between 6 cm⁻¹ and 176 cm⁻¹. We find that the various conformers of acrylic acid can be identified by a double peak for the C=O and O–H vibrations, which have $\Delta\nu^0$ and $\Delta\nu^{00}$ values of 24 and 42 cm⁻¹, respectively. Our study reveals important new findings about the spectroscopic identification of the various conformers of lactic and acrylic acid and the effect that intra-molecular hydrogen bonding in L-lactic acid can have on the dehydration mechanism occurring in potassium substituted NaY zeolites.

Conflicts of interest

The authors declare no conflicts of interest.

Acknowledgements

The authors wish to acknowledge the provision of financial support through EPSRC grants EP/L02537X/1 and EP/L026317/1. The authors acknowledge the use of the Grace High Performance Computing Facility (Grace@UCL), and associated support services, in the completion of this work.

References

- 1 H. Benninga, *A History of Lactic Acid Making: A Chapter in the History of Biotechnology*, Kluwer Academic Publishers, London, 1990.
- 2 M. Kleerebezem and J. Hugenholtz, *Curr. Opin. Biotechnol.*, 2003, 14, 232–237.
- 3 A. J. Domb, N. Kumar, T. Sheskin, A. Bentolila, J. Slager and T. Teomim, *Polymeric biomaterials*, Marcel Dekker, New York, 2001.
- 4 J. Jem, J. van der Pol and S. de Vos, *Microbiol. Monographs*, 2010, 14, 323–346.
- 5 H. Danner, M. Urmos, M. Gartner and R. Braun, *Appl. Biochem. Biotechnol.*, 1998, 70-72, 887–894.
- 6 J. Peng, X. Li, C. Tang and W. Bai, *Green Chem.*, 2014, 16, 108–111.
- 7 C. T. Lira and P. J. McCrackin, *Ind. Eng. Chem. Res.*, 1993, 32, 2608–2613.
- 8 R. A. Sawicki, *Catalyst for Dehydration of Lactic Acid to Acrylic Acid*, US Pat., 4729978, 1988.
- 9 C. Paperizos, W. G. Shaw and S. R. Dolhyj, *Catalytic Conversion of Lactic Acid and Ammonium Lactate to Acrylic Acid*, Eur. Pat., 85307642.0, 1985.
- 10 P. Sun, D. Yu, Z. Tang, H. Li and H. Huang, *Ind. Eng. Chem. Res.*, 2010, 49, 9082–9087.
- 11 B. P. van Eijck, *J. Mol. Spectrosc.*, 1983, 101, 133–138.
- 12 K. E. Norris and J. E. Gready, *THEOCHEM*, 1992, 258, 109–138.
- 13 K. E. Norris and J. E. Gready, *THEOCHEM*, 1993, 279, 99–125.

- 14 A. Borba, A. Go´mez-Zavaglia, L. Lapinskic and R. Fausto, *Phys. Chem. Chem. Phys.*, 2004, 6, 2101–2108.
- 15 I. D. Reva, S. Jarmelo, L. Lapinski and R. Fausto, *Chem. Phys. Lett.*, 2004, 389, 68–74.
- 16 S. Jarmelo, D. A. S. Marques, P. N. Simoˆes, R. A. Carvalho, C. M. S. G. Batista, C. Araujo-Andrade, M. H. Gil and R. Fausto, *J. Phys. Chem. B*, 2012, 116, 9–21.
- 17 S. Banerjee, S. K. Bhanja and P. Kanti Chattopadhyay, *Comput. Theor. Chem.*, 2018, 1125, 29–38.
- 18 M. J. Frisch, G. W. Trucks, H. B. Schlegel, G. E. Scuseria, M. A. Robb, J. R. Cheeseman, G. Scalmani, V. Barone, G. A. Petersson, et al., *Gaussian 09*, Gaussian Inc., Wall-ingford CT, 2009.
- 19 A. D. Becke, *J. Chem. Phys.*, 1993, 98, 5648.
- 20 C. Lee, W. Yang and R. G. Parr, *Phys. Rev. B: Condens. Matter Mater. Phys.*, 1988, 37, 785–789.
- 21 C. D. Zeinalipour-Yazdi, A. L. Cooksy and A. M. Efstathiou, *Surf. Sci.*, 2008, 602, 1858–1862.
- 22 C. D. Zeinalipour-Yazdi and R. A. van Santen, *J. Phys. Chem. C*, 2012, 116, 8721–8730.
- 23 C. D. Zeinalipour-Yazdi, D. J. Willock, L. Thomas, K. Wilson and A. F. Lee, *Surf. Sci.*, 2016, 646, 210–220.
- 24 D. E. Woon and T. H. Dunning Jr., *J. Chem. Phys.*, 1993, 98, 1358.
- 25 A. Wilson, T. van Mourik and T. H. Dunning Jr., *J. Mol. Struct.*, 1997, 388, 339–349.
- 26 K. A. Peterson, D. E. Woon and T. H. Dunning Jr., *J. Chem. Phys.*, 1994, 100, 7410.
- 27 R. A. Kendall, T. H. D. Jr and R. J. Harrison, *J. Chem. Phys.*, 1992, 96, 6796.
- 28 T. H. Dunning Jr., *J. Chem. Phys.*, 1989, 90, 1007.
- 29 J. L. McHale, *Molecular Spectroscopy*, Prentice Hall, Upper Saddle River NJ, 1999.
- 30 A. Schouten, J. A. Kanters and J. van Krieken, *J. Mol. Struct.*, 1994, 323, 165–168.
- 31 C. Hammaeher and J.-F. Paul, *J. Catal.*, 2013, 300, 174–182.
- 32 L. Pauling, *J. Am. Chem. Soc.*, 1932, 54, 3570–3582.
- 33 S. E. Stein, in *Infrared Spectra in NIST Chemistry WebBook*, NIST Standard Reference Database Number 69, ed. P. J. Linstrom and W. G. Mallard, National Institute of Standards and Technology, Gaithersburg MD, 20899, retrieved July 20, 2018.
- 34 V. Mohacek-Grosev, V. Sostaric and A. Maksimovic, *Spectrochim. Acta, Part A*, 2015, 140, 35–43.
- 35 G. Cassanas, M. Morssli, E. Fabregue and L. Bardet, *J. Raman Spectrosc.*, 1991, 22, 409–413.
- 36 M. Losada, H. Tran and Y. Xu, *J. Chem. Phys.*, 2008, 128, 014508.
- 37 M. N. Zhang Yu and W. Wei-Zhou, *Acta Phys.-Chim. Sin.*, 2012, 28, 499–503.
- 38 J. Grabska, M. Ishigaki, K. B. Bec´, M. J. Wo´jcik and Y. Ozaki, *J. Phys. Chem. A*, 2017, 121, 3437–3451.
- 39 S. Ostrowski, M. E. Jamro´z and J. C. Dobrowolski, *Comput. Theor. Chem.*, 2011, 974, 100–108.
- 40 R. J. Loncharich, T. R. Schwartz and K. N. Houk, *J. Am. Chem. Soc.*, 1987, 109, 14–23.
- 41 K. Bolton, N. L. Owen and J. Sheridan, *Nature*, 1968, 218, 266.
- 42 K. Bolton, D. G. Lister and J. Sheridan, *J. Chem. Soc., Faraday Trans.*, 1974, 70, 113.
- 43 J. Umemura and S. Hayashi, *Bull. Inst. Chem. Res., Kyoto Univ.*, 1974, 52, 585.
- 44 W. R. Fairheller Jr. and J. E. Katon, *Spectrochim. Acta, Part A*, 1967, 23, 2225.
- 45 S. W. Charles, F. C. Cullen, N. L. Owen and G. A. Williams, *J. Mol. Model.*, 1987, 157, 17–29.